Supplementary Material

S1: Details on the used polymers in the carried out experiments and simulations

Table S1. Properties of the seven abundant polymers used in this study.

Polymer name	Abbreviation	Structure	Density (gcm^{-3})	Type
Polystyrene	PS	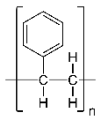	1.030	Non-biodegradable
Polyamide 66	PA66	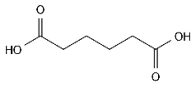	1.12	Non-biodegradable
Polycaprolacton	PCL	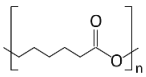	1.14	Biodegradable
Polylactic acid	PLA		1.20	Biodegradable
Poly(L-lactic acid)	PLLA	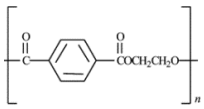	1.20	Biodegradable
Polybutylenadipate terephthalate	PBAT	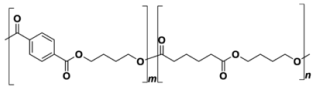	1.22	Non-biodegradable
Polyvinyl chloride	PVC	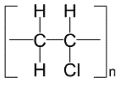	1.38	Non-biodegradable

S2: Adjusted initial and boundary conditions in all the conducted simulations

Table S2. The used initial and boundary conditions in the simulations conducted by OpenFOAM.

		Velocity	Pressure	Phase Saturation
Upper wall	type	inletOutlet;	fixedValue;	fixedValue;
	value	internalField	internalField	uniform 0;
MP particle	type	movingWallVelocity	fixedFluxPressure;	zeroGradient;
	value	internalField	-	-
Side walls	type	fixedValue	fixedFluxPressure;	zeroGradient;
	value	internalField	-	-
Lower wall	type	fixedValue	fixedFluxPressure;	zeroGradient;
	value	internalField	-	-

S3: Calculation of MOI for an arbitrary particle

The following equations are used to calculate mass (m) and mass moment of inertia (I_o) of particle with arbitrary shape (Ehrlich and Weinberg, 1970; Peraire and Widnall, 2008; Tang and Shangguan, 2011) (Figure S1) in which r_i is a vector that points out to the position of the i^{th} cell in the mesh of a designed particle within a Cartesian coordinate system and $\rho\ (r_i)$ is the particle density in the i^{th} cell:

$$m = \int_{v_{(r)}} \rho\ (r_i)\ dV(\vec{r}) \tag{1}$$

$$I_o = \int_{v_{(r)}} \rho\ (r_i)\ r_i^2 dV(\vec{r}) = \int \begin{bmatrix} x_i^2 + y_i^2 & -x_i y_i & -x_i z_i \\ -x_i y_i & x_i^2 + y_i^2 & -y_i z_i \\ -x_i z_i & -y_i z_i & x_i^2 + y_i^2 \end{bmatrix} \rho\ (r_i)\, dV(\vec{r}) \tag{2}$$

Origin is the rotational axis of the particle's moment of inertia which is calculated by equation 2. Having the coordinate of the particle's center of mass ($\vec{c}$) (equation 3) and using the parallel axes theorem, MOI of the particles around their center of gravity can be calculated using equation 4.

$$\vec{c} = \frac{1}{m} \int_{v_{(r)}} \vec{r}_i\ \ \rho\ (r_i)\, dV(\vec{r}) \tag{3}$$

$$I_o = \int \begin{bmatrix} x_i^2 + y_i^2 & -x_i y_i & -x_i z_i \\ -x_i y_i & x_i^2 + y_i^2 & -y_i z_i \\ -x_i z_i & -y_i z_i & x_i^2 + y_i^2 \end{bmatrix} \rho\ (r_i)\, dV(\vec{r}) - \int_{v_{(r)}} \rho\ (r_i)\ dV(\vec{r}) \begin{bmatrix} C_y^2 + C_z^2 & -C_x C_y & -C_x C_z \\ -C_x C_y & C_x^2 + C_z^2 & -C_y C_z \\ -C_x C_z & -C_y C_z & C_x^2 + C_y^2 \end{bmatrix} \tag{4}$$

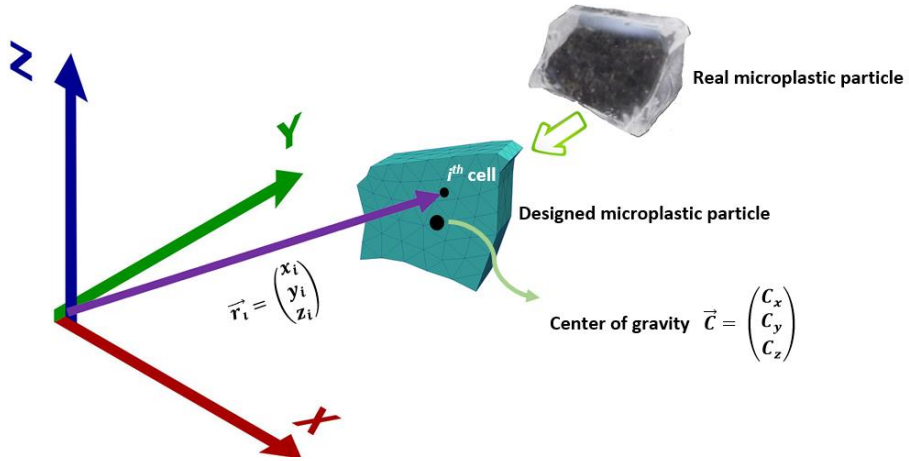

Figure S1. Position vector and center of mass location of an irregularly shaped MP particle.

S4: A number of the designed irregularly shaped MP particles and their real images

Table S3. Some of the designed particles based on the shape of real irregularly shaped MP particles.

Polymer type	Real MP particle	Simulated MP particle	Polymer type	Real MP particle	Simulated MP particle
PLLA			PA66		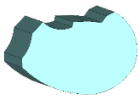
					
					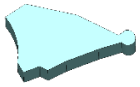
PCL			PBAT		
					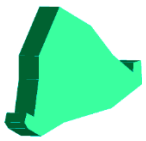
					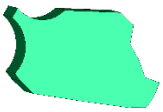
PS			PVC		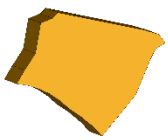
					

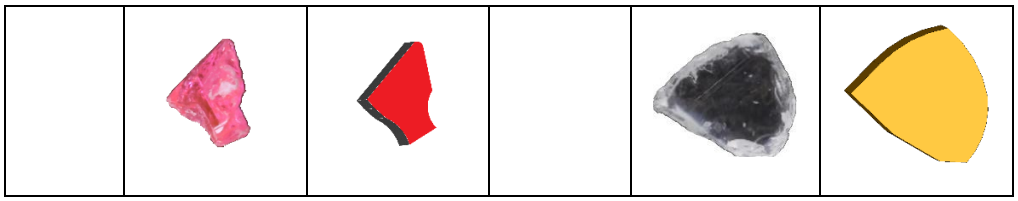

In the table a selection of the real MP particles used in the experiments and their designed shapes using the meshing software SALOME 9.4 software (Ribes and Caremoli, 2007) are depicted. The simulation results for three random particles software are visualized using ParaView software (Ahrens et al., 2005) (see supplementary animation (Video 1)). In order to compare their sizes in the interpretations, equation 5 was used to calculate the diameter of spheres with volumes identical to the volumes of the MP particles.

$$D_{eq} = \sqrt[3]{ABC} \tag{5}$$

A and C are the longest and shortest lengths of each particle and B is the arithmetic average of A and C (Kooi et al., 2016; Waldschläger and Schüttrumpf, 2019).

S5: Calculating side length of the polygons with identical areas to generate particles of the same volumes

A regular polygon with N sides is a cyclic polygon which is described using two circles, an inscribed circle that forms the tangent to the middle points of all sides of a regular polygon, and a circumscribed circle which passes through all its vertices. As the number of sides of a polygon increase towards infinity, the lengths of its sides converge to zero, so that the inscribed and circumscribed circles eventually overlap. Knowing the side length and the number of sides, equation 6 returns the area of a regular polygon. Figure S2 has been drawn based on equation 6 so that considering areas equal to circles with diameters of 0.5 mm, 1mm, 1.5mm, 2mm, and 2.5mm, the side length (a) of the polygons with areas equal to their corresponding circles were calculated.

$$A = \frac{1}{4}\, n a^2 \cot\frac{\pi}{n} \tag{6}$$

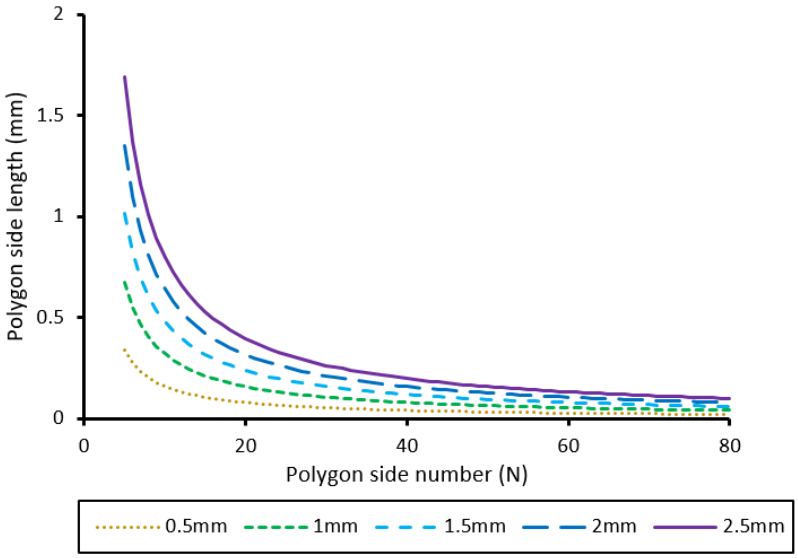

Figure S2. The side lengths of regular 2D polygons with areas identical to a circle derived from a polygon with an infinite number of sides (legend shows the diameters of the circles).

S6. Behavior of a particle before and after reaching its terminal settling velocity (TSV)

Figure S3-A illustrates the evolution of the settling velocity in the initial transient phase of settling for four particles with different shapes, which show different, shape-dependent behavior. Figure S3-B shows the velocity evolution for 5 triangular particles entering the water column with different orientations at angles of 45°, 90°, 135°, and 180°. The velocity evolution in the transient phase of settling before reaching a constant terminal settling velocity (TSV) clearly dependents on the orientation of the particle when entering the water column (Figure S3-B). In this transient phase the settling velocity can fluctuate around the TSV as a result of secondary oscillating, rotating and tumbling movements of the MP particles. Those types of secondary movements were also observed in the settling experiments in the present as well as other studies (Khatmullina and Isachenko, 2017).

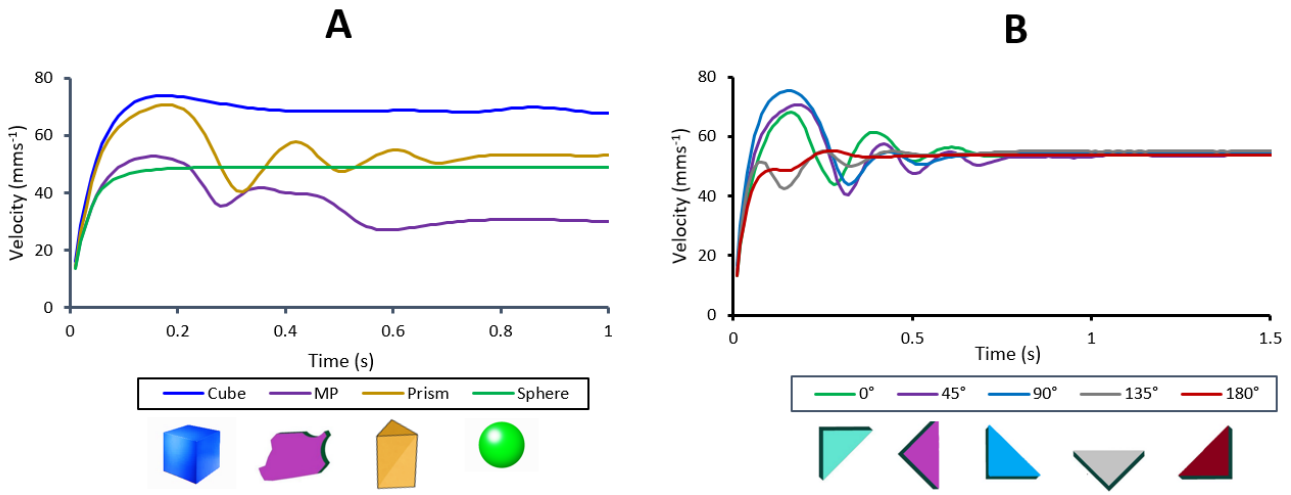

Figure S3. Velocity profile before and after reaching TSV for (A) three different regular particles (cube, prism, and sphere) and an irregular MP particle, (B) Evolution of the settling velocity of a triangular particle entering the water column with orientations at different angles (0°,45°, 90°, 135°, 180°).

References

Ahrens, J., Geveci, B., and Law, C. (2005). Paraview: An end-user tool for large data visualization. *The visualization handbook* 717(8).

Ehrlich, R., and Weinberg, B. (1970). An exact method for characterization of grain shape. *Journal of sedimentary research* 40(1)**,** 205-212.

Khatmullina, L., and Isachenko, I. (2017). Settling velocity of microplastic particles of regular shapes. *Marine pollution bulletin* 114(2)**,** 871-880.

Kooi, M., Reisser, J., Slat, B., Ferrari, F.F., Schmid, M.S., Cunsolo, S., et al. (2016). The effect of particle properties on the depth profile of buoyant plastics in the ocean. *Scientific reports* 6(1)**,** 1-10.

Peraire, J., and Widnall, S. (2008). Lecture L26-3D Rigid Body Dynamics: The Inertia Tensor. *Dynamics*.

Ribes, A., and Caremoli, C. (Year). "Salome platform component model for numerical simulation", in: *31st annual international computer software and applications conference (COMPSAC 2007)*: IEEE), 553-564.

Tang, L., and Shangguan, W.-B. (2011). An improved pendulum method for the determination of the center of gravity and inertia tensor for irregular-shaped bodies. *Measurement* 44(10)**,** 1849-1859.

Waldschläger, K., and Schüttrumpf, H. (2019). Effects of particle properties on the settling and rise velocities of microplastics in freshwater under laboratory conditions. *Environmental science & technology* 53(4)**,** 1958-1966.